J|A|C|S COMMUNICATIONS

Published on Web 10/20/2009

Synthesis of SnS Quantum Dots

Ying Xu,[†] Najeh Al-Salim,[‡] Chris W. Bumby,[†] and Richard D. Tilley*,[†]

School of Chemical and Physical Sciences and the MacDiarmid Institute of Advanced Materials and Nanotechnology, Victoria University of Wellington, P.O. Box 600, Wellington, New Zealand, and Industrial Research, Ltd., P.O. Box 31-310, Lower Hutt, New Zealand

Received August 11, 2009; E-mail: richard.tilley@vuw.ac.nz

Narrow band gap IV−VI semiconductor nanoparticles (NPs) such as PbS, SnTe, and SnS that are optically active in the near-infrared (NIR) and infrared (IR) are of great interest for their applications in photovoltaics, near-infrared detectors, and biomedical applications such as hyperthermia where strong IR absorption is required.[1] These applications have stimulated the search for convenient synthetic methodologies to make SnS NPs with narrow size distributions and well-defined optical properties.

In the past decade, much attention has been given to the synthesis of monodispersed chalcogenide nanoparticles with cubic structures such as CdS, CdSeS, CdSe, PbS, and SnTe due to their ease of synthesis.[2] SnS adopts an orthorhombic layered crystal structure that can be considered as a distorted NaCl structure.[3] The synthesis of uniform size IV−VI semiconductor NPs with layered structures that are small enough to be in the quantum confinement regime is still a significant challenge.

There are only a few reports that present synthetic methodologies for forming SnS NPs.[4] To our knowledge there is only one report by Hickey et al. demonstrating a method of forming SnS NPs less than 10 nm in size and none with sizes less than 7 nm.[5] The synthesis of Hickey and co-workers uses the air sensitive organometallic complex $Sn[N(SiCH_3)_2]_2$ as a tin precursor. The reaction uses ligands which render the nanocrystals hydrophobic.[5]

Here we report a facile, room temperature, synthesis to make hydrophilic SnS NPs of only a few nanometers in size. The nanoparticles were made in solution using ionic starting materials $SnBr_2$ and Na_2S in the presence of various ethanolamines (EAs) in ethylene glycol. The ethanolamine ligands used had three hydroxyl groups (triethanolaime (TEA)), two hydroxyl groups (*N*-methyldiethanolamine (MDEA)), or one hydroxyl group (*N*,*N*-dimethylethanolamine (DMEA)) (see Supporting Information for full synthesis details).

The smallest and most monodisperse SnS NPs were formed using TEA as the stabilizing ligand. A typical transmission electron microscope (TEM) image of the reaction product synthesized using TEA is shown in Figure 1a and shows that the nanoparticles are approximately spherical in shape. The inset, Figure 1b, shows an HRTEM image of an individual nanocrystal with the atomic lattice fringes clearly visible, demonstrating the highly crystalline nature of the SnS NPs. A histogram showing the nanoparticle size distribution taken from over 110 nanoparticles is shown in Figure 1c and indicates an average nanoparticle size of 3.2 nm ± 0.5 nm. When MDEA was used as the stabilizing ligand in the reaction, nanoparticles of sizes 4.0 nm ± 2.0 nm were formed. When DMEA was used, nanoparticles with average sizes of 5.0 nm ± 4.0 nm were produced (see Supporting Information SI 1a−d).

The results show that nanoparticle size and monodispersity can be controlled by the number of hydroxyl groups on the stabilizer.

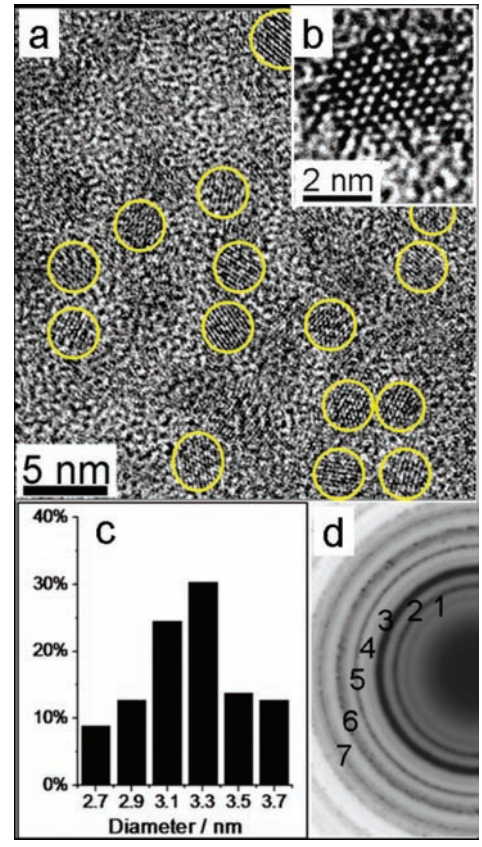

Figure 1. (a and b) TEM images showing crystalline SnS NPs obtained with TEA, (c) histogram of nanoparticle size distribution, (d) selected area electron diffraction (SAED) pattern of orthorhombic SnS NPs.

TEA (three hydroxyl groups) produced smaller and more monodisperse nanoparticles than MDEA (two hydroxyl groups) which in turn formed smaller and more monodisperse nanoparticles than DMEA (one hydroxyl group). The greater monodispersity with the increasing number of hydroxyl groups most likely arises from the ability of multiple hydroxyl groups to bind more strongly to the nanocrystals as they grow.

Previous reports show that TEA complexes with Sn^{2+} to form a chelate compound $[Sn(TEA)_n]^{2+}$.[6] A proposed reaction for the formation of SnS is illustrated in Scheme 1 proceeding via an $[Sn(TEA)_n]^{2+}$ intermediate. DMEA and MDEA also form complexes with tin that are less stable than the TEA complex.[6]

The selective-area electron diffraction (SAED) pattern, Figure 1d, has a sharp set of diffraction rings. These diffraction rings match and can be indexed to the planes of orthorhombic phase SnS (*Pbnm*, $a = 11.143$ Å, $b = 3.971$ Å, and $c = 4.336$ Å. 1-(101); 2-(201), (210); 3-(011), (111), (301), (400); 4-(211), (401); 5-(311), (410);

[†] Victoria University of Wellington.
[‡] Industrial Research, Ltd.

10.1021/ja906804f CCC: $40.75

Scheme 1. Schematic Illustration of the Formation of SnS NPs

$$Sn^{2+} + nTEA \rightleftharpoons [Sn(TEA)_n]^{2+} \quad (1)$$

$$[Sn(TEA)_n]^{2+} + S^{2-} \longrightarrow SnS + nTEA \quad (2)$$

6-(102), (020), (501), (112); and 7-(121), (511)). No cubic phase SnS was detected, which was further confirmed by powder X-ray diffraction (see Supporting Information SI 2).

Energy-dispersive X-ray (EDX) analysis of the chemical composition SnS NPs showed an atomic ratio of Sn to S of 1.0:1.0, consistent with SnS (see Supporting Information SI 3).

Reflectivity measurements were made upon drop-cast films of nanoparticles deposited on glass substrates. Figure 2a shows the reflectivity data for films of the three nanoparticle samples. The smaller and more monodisperse samples produced using TEA and MDEA show a reflectivity edge that is blue-shifted by ~0.4 eV compared to the DMEA sample. The inset plot shows the first derivative of reflectivity with respect to incident photon energy, $h\nu$; peaks in these data correspond to the reflectivity edge of the semiconductor nanocrystals. The TEA and MDEA samples exhibit reflectivity edges of ~1.65 eV. This value is significantly higher than the 1.1 eV reported for the bulk band gap of SnS and comparable to 1.6 eV reported for ~7 nm SnS NPs.[5,7] In addition the more monodisperse TEA sample has a narrower peak than the MDEA sample. These observations can be explained by quantum effects arising from changes to the SnS band structure that occur in nanocrystals with a small diameter. In contrast the DMEA sample exhibits two peaks in the reflectance derivative at ~1.6 and ~1.2 eV. This result is most likely due two populations of nanoparticles in this sample, those with diameters above 6.5 nm that exhibit behavior similar to bulk SnS (peak at ~1.2 eV) and those with diameters below 6.5 nm (peak at ~1.6 eV).

Figure 2b shows UV−vis−NIR optical absorption data. Transmission measurements were performed upon colloidal nanoparticle dispersions in ethanol that were translucent brown in color (inset, Figure 2b). The solutions exhibit continuous absorption across the UV−vis spectrum, with increasing absorption near the UV region (see Supporting Information). For a sample behaving like a bulk indirect semiconductor, the absorption coefficient, α, can be described by the relationship $\alpha^{0.5} \propto$ photon energy, $h\nu$.[8] This relationship is valid close to the indirect band gap edge where the single parabolic band approximation holds. An estimate of the indirect band gap (E_g) of sample can also be obtained from the intercept of this plot.[8] Figure 2b shows that the DMEA sample exhibits a clear region of linearity in $(\alpha h\nu)^{0.5}$ vs $h\nu$ and an estimated indirect band gap $E_g \approx 1.1$ eV, indicating the presence of larger SnS particles with optical characteristics similar to those of bulk material. Comparison with data from an amorphous SnS bulk film shows similar features to those the DMEA sample.[7] There is no region of linearity observed for the smaller TEA and MDEA samples. This is as expected for quantum dots exhibiting a 0-D joint density of states and again illustrates that the nanocrystals are small enough to be in the quantum confinement regime. No fluorescence was observed from the sample consistent with indirect semiconductor behavior.

After purification, the surface of the SnS NPs was characterized by FTIR spectroscopy and showed the presence of EA capping ligands (see Supporting Information SI 4). The SnS NPs are readily dispersed in water for biomedical applications and other polar solvents for the incorporation of the IR-sensitive SnS NPs into biphase polymer blends for photovoltaic devices.

In summary, colloidal SnS NPs of ~4 nm with narrow size distributions have been synthesized using ethanolamine ligands.

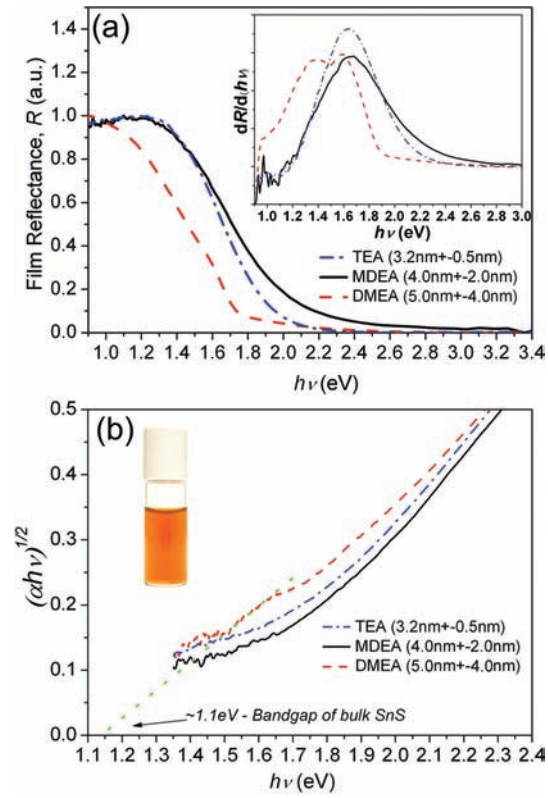

Figure 2. Optical properties of SnS NPs: (a) Optical reflectance spectra of nanoparticle films. Inset: First derivative of film reflectance vs incident photon energy; (b) The dependence of $\alpha^{0.5}$ on photon energy ($h\nu$) and inset a photograph of SnS NPs dispersed in ethanol solution.

Optical studies of the SnS NPs show size dependent effects in both absorbance and reflectivity. This work unlocks the use of water-soluble SnS NPs for biomedicine and photovoltaics.

Acknowledgment. Y.X., N.A., C.W.B., and R.D.T. thank FRST for funding through Grant IIOF VICX0601.

Supporting Information Available: Details of the synthesis, TEM, XRD, EDX, and FTIR analysis. This material is available free of charge via the Internet at http://pubs.acs.org.

References

(1) (a) Rauch, T.; Böberl, M.; Tedde, S. F.; Fürst, J.; Kovalenko, M. V.; Hesser, G.; Lemmer, U.; Heiss, W.; Hayden, O. *Nat. Photonics* **2009**, *3*, 332. (b) Souici, A. H.; Keghouche, N.; Delaire, J. A.; Remita, H.; Etcheberry, A.; Mostafavi, M. *J. Phys. Chem. C* **2009**, *113*, 8050.
(2) (a) Washington, A. L., II; Strouse, G. F. *J. Am. Chem. Soc.* **2008**, *130*, 8916. (b) Al-Salim, N.; Young, A. G.; Tilley, R. D.; McQuillan, A. J.; Xia, J. *Chem. Mater.* **2007**, *19*, 5185. (c) Xu, S.; Kumar, S.; Nann, T. *J. Am. Chem. Soc.* **2006**, *128*, 1054. (d) Lu, W.; Fang, J.; Stokes, K. L.; Lin, J. *J. Am. Chem. Soc.* **2004**, *126*, 11798. (e) Kovalenko, M. V.; Heiss, W.; Shevchenko, E. V.; Lee, J.-S.; Schwinghammer, H.; Alivisatos, A. P.; Talapin, D. V. *J. Am. Chem. Soc.* **2007**, *129*, 11354.
(3) Chamberlain, J. M.; Nikolic, P. M.; Merdan, M.; Mihailovic, P. *J. Phys. C: Solid State Phys.* **1976**, *9*, L637.
(4) (a) Greyson, E. C.; Barton, J. E.; Odom, T. W. *Small* **2006**, *2*, 368. (b) Koktysh, D. S.; McBride, J. R.; Rosenthal, S. J. *Nano. Res. Lett.* **2007**, *2*, 144. (c) Schlecht, S.; Kienle, L. *Inorg. Chem.* **2001**, *40*, 5719.
(5) Hickey, S. G.; Waurisch, C.; Rellinghaus, B.; Eychmuller, A. *J. Am. Chem. Soc.* **2008**, *130*, 14978.
(6) Pramanik, P.; Basu, K.; Biswas, S. *Thin Solid Films* **1987**, *150*, 269.
(7) (a) Thangaraju, B.; Kaliannan, P. *J. Phys D: Appl. Phys.* **2000**, *33*, 1054. (b) Albers, W.; Haas, C.; van der Maesen, F. *J. Phys. Chem. Solids* **1960**, *15*, 306.
(8) (a) Hagfeldt, A.; Gratzel, M. *Chem. Rev.* **1995**, *95*, 49. (b) Li, X.; Li, J. G.; Huo, D.; Xiu, Z.; Sun, X. *J. Phys. Chem. C* **2009**, *113*, 1806. (c) Pradhan, D.; Leung, K. T. *Langmuir* **2008**, *24*, 9707.

JA906804F